Available online at www.sciencedirect.com
ScienceDirect
Applied Energy 84 (2007) 1–15
APPLIED ENERGY
www.elsevier.com/locate/apenergy

Modelling and experimental verification of the operating current of mono-crystalline photovoltaic modules using four- and five-parameter models

Ali Naci Celik *, Nasır Acikgoz

Mustafa Kemal University, Faculty of Engineering and Architecture, Mechanical Engineering Department, 31024 Antakya, Hatay, Turkey

Available online 19 June 2006

Abstract

This article presents the modelling and experimental verification of the operating current of a 120 W of mono-crystalline photovoltaic module using four- and five-parameter analytical models. The southern part of Turkey, where the experimental system is mounted, is particularly well suited to photovoltaic installations. The operating current of the photovoltaic module, calculated from the models, is validated based on a series of experimental measurements. As well as the current and voltage of the photovoltaic module, the environmental variables such as ambient temperature and solar irradiance were measured and used for validation of the operating current. The photovoltaic cell models considered in this article are drawn from the equivalent electrical circuit that includes light-generated current, diode reverse saturation current, and series and shunt resistances. The simplified four-parameter model assumes the shunt resistance as infinite and thus neglects it. After determining the model parameters, the operating current is calculated using both models and compared to the measured current produced by the photovoltaic module. It is shown that the complete five-parameter model predicts the operating current better than the simplified four-parameter model, especially around solar noon, when most of the power is produced.

Keywords: Photovoltaic cell models; Four- and five-parameter photovoltaic cell models; Calculation of operating photovoltaic current

* Corresponding author. Tel.: +90 326 2455836x1438; fax: +90 326 2455499.
E-mail address: ancelik@hotmail.com (A.N. Celik).

0306-2619/$ - see front matter © 2006 Elsevier Ltd. All rights reserved.
doi:10.1016/j.apenergy.2006.04.007

Nomenclature

a	curve-fitting parameter for the four-parameter model; defined as $a = mV_t$
a_{ref}	curve-fitting parameter for the four-parameter model at reference condition
A	module area (m^2)
AM	air mass
E_q	energy-band gap (eV)
G	solar irradiance (W/m^2)
G_{ref}	solar irradiance at reference condition (W/m^2)
I	current of the module (A)
I_L	light-generated current (A)
$I_{L,ref}$	light-generated current at reference condition (A)
I_{mp}	current at maximum-power point (A)
$I_{mp,ref}$	current at maximum-power point at reference condition (A)
I_o	diode reverse saturation-current (A)
$I_{o,ref}$	diode reverse saturation-current at reference condition (A)
I_{sc}	short-circuit current (A)
$I_{sc,ref}$	short-circuit current at reference condition (A)
k	Boltzmann's constant ($1.3806505 \times 10^{-23}$ J K^{-1})
m	ideality factor; defined as $m = N_s n_I$
n_I	diode ideality factor
N_s	number of cells in series in one module
P	power of the module (W)
P_{max}	power at maximum-power point (W)
$P_{mp,ref}$	power at maximum-power point at reference condition (W)
q	electron charge (1.60218×10^{-19} C)
R_s	series resistance (Ω)
$R_{s,ref}$	series resistance at reference condition (Ω)
R_{sh}	shunt resistance (Ω)
R_{sho}	reciprocal of slope at short-circuit point (Ω)
R_{so}	reciprocal of slope at open-circuit point (Ω)
T_c	cell temperature (K)
$T_{c,ref}$	cell temperature at reference condition (K)
V	voltage of the module (V)
V_{mp}	voltage at maximum power point (V)
$V_{mp,ref}$	voltage at maximum-power point at reference condition (V)
V_{oc}	open-circuit voltage (V)
$V_{oc,ref}$	open-circuit voltage at reference condition (V)
V_t	thermal voltage (V)
η	efficiency of the module at maximum-power point
$\mu_{V,oc}$	temperature coefficient of open-circuit voltage (V/K)
$\mu_{I,sc}$	temperature coefficient of short-circuit current (A/K)

1. Introduction

The need for an increasing use of photovoltaic energy systems is acknowledged throughout the world [1]. The global installed capacity of photovoltaic systems in 2003 grew to 1809 MW [2]. Approximately 48% of the total, or 860 MW, was installed in Japan. More than 80% of this capacity was installed in residential photovoltaic systems. Germany, however, had taken the lead in the residential use of photovoltaics with the initiation of the 1000 roof program in the early 1990s. This program was intended to subsidise the installation of 1000 photovoltaic systems, each of a few kilowatts rating, on the roofs of private residences with the systems being owned by private individuals, but with appreciable government subsidies (50–70%) [3]. Furthermore, in 1999, the German government implemented another program to encourage the installation of 100,000 roofs by 2004. Global photovoltaic module shipments grew to about 744 MW in 2003, an increase of 32.5% compared with the preceding year [2]. Japan produced 364 MW, or almost one-half of global photovoltaic module shipments. Japan has also set a domestic target for installed capacity of photovoltaic-power generation systems as 4.82 GW by 2010 [2].

This high growth rate has led to an increase in research projects on various aspects of photovoltaics, from the development of novel photovoltaic cells [4,5] to the performance analysis, sizing, performance estimation and optimisation of photovoltaic energy systems [6–10]. Modelling of photovoltaic cells is an essential topic of research. Photovoltaic cell models are usually drawn from the equivalent electrical-circuit as either four or five-parameter models. The complete five-parameter model consists of light-generated current, diode reverse saturation-current, series resistance, shunt resistance and diode ideality factor [11,12]. The simplified four-parameter model assumes the shunt resistance as infinite and it is neglected [13]. Some other models that describe the behaviour of a photovoltaic module or the energy produced from it, based on empirical approaches, are studied elsewhere [14,15]. As well as the characteristic parameters, the performance of a photovoltaic module is dependent on the climatic conditions of the location. The technical data provided by the manufacturers may not necessarily describe the performance of photovoltaic modules at a particular site because the climatic conditions can differ dramatically from the standard test-conditions. This may lead to over or under estimation of energy production in real working conditions. Indeed an overestimation of the production by up to 40% was reported in comparison to the production in Standard Test Conditions [15]. Therefore, the knowledge of important characteristics of photovoltaic modules under real operating conditions is of great importance for determining their performance.

This article presents the modelling and experimental verification of the operating current of a 120 W of mono-crystalline photovoltaic module using four- and five-parameter analytical models. The southern part of Turkey, where the experimental system is mounted, is particularly well suited to photovoltaic installations. The operating current of the photovoltaic module predicted from the models is validated based on a series of experimental measurements. In spite of the fast growth rate of photovoltaic energy systems in the world, the total installed photovoltaic power capacity in Turkey is estimated to be around 300 kW. The potential in Turkey as a photovoltaic market is very large, since the country abounds in solar radiation and large areas of available land for solar farms. There are more than 30,000 small residential areas where solar powered electricity would

likely be more economical than extending the grid electricity, as well as holiday villages at the long coastal areas [16]. However, research on photovoltaic cells and photovoltaic energy systems that helps propagate this technology in Turkey has been rather limited [17,18].

2. Photovoltaic modules and the experimental set-up

The experimental system consists of 120 W of mono-crystalline photovoltaic modules situated on the top of a building in Iskenderun (36.35°N; 36.10°E), located on the eastern Mediterranean coast of Turkey. The modules were mounted tilted at an angle that is equal to the latitude of the location, facing due south. Fig. 1 shows the photovoltaic modules situated on the roof of the building. Technical characteristics of the photovoltaic modules used for modelling are as follows: short-circuit current at reference condition $I_{sc,ref} = 7.7$ A, open-circuit voltage at reference condition $V_{oc,ref} = 21$ V, current at maximum-power point at reference condition $I_{mp,ref} = 7.1$ A, voltage at maximum-power point at reference condition $V_{mp,ref} = 16.9$ V, power at maximum-power point at reference condition $P_{mp,ref} = 120$ W. These are provided by the manufacturer for the reference conditions of 1000 W/m^2 of irradiance level, 25 °C of cell temperature, and 1.5 of air mass (AM), which is the ratio of the mass of air that the beam radiation has to traverse at any given time and location to the mass of air that the beam radiation would traverse if the sun were directly overhead [11]. The photovoltaic modules under study are made up of 36 cells connected in series, each of 0.027 m^2, adding up to a total area of 0.974 m^2. The electron-band gap E_q is 1.124 eV for this mono-crystalline silicon photovoltaic module.

The layout of the experimental system is presented in Fig. 2. As well as the photovoltaic modules, the experimental system consists of 200 Ah/12 V sealed type lead-acid battery and a DC/AC inverter of 600 W/12 V and 230 V/50 Hz, with a maximum efficiency of

Fig. 1. Photovoltaic modules mounted at an angle of 36° situated on the top of a building in Iskenderun, Turkey.

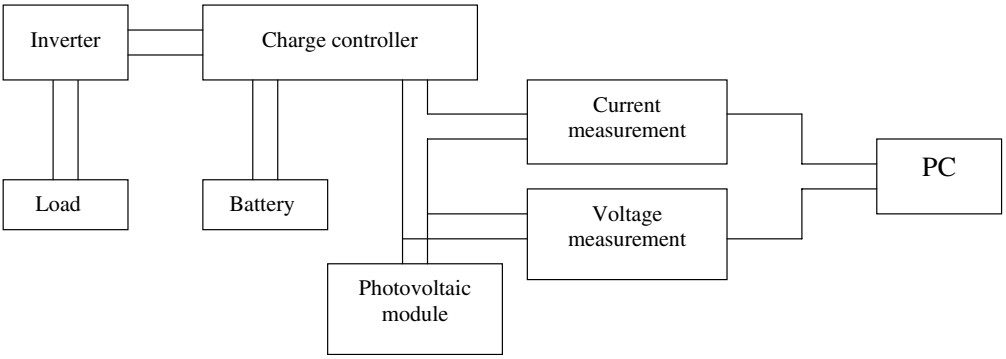

Fig. 2. Layout of the experimental system.

98%. The load connected to the photovoltaic system is a number of light bulbs, whose power varies between 0 and 200 W depending on the state of charge of the battery. The photovoltaic modules are connected to the battery and the load through an inverter and a charge controller. The experimental verification of the models was carried out under real working condition of the photovoltaic system. The current and voltage of the photovoltaic modules were measured at 30-s intervals by current and voltage sensors, respectively. The measurements were stored in data loggers and averaged further as required.

3. Photovoltaic-cell models

There exist several mathematical models in the literature to describe photovoltaic cells, from simple to more complex models ranging that account for different reverse saturation currents. The two-diode equations with the saturation currents I_{o1} and I_{o2} and with the diode factors n_1 and n_2 describe diffusion and recombination characteristics of the charge carriers in the material itself and in the space-charge zone [19]. To simplify parameter adjustment, the two-diode model can be reduced to a one-diode model in which, according to the Shockley theory, recombination in the space-charge zone is neglected, so the second diode term is omitted [19].

An electrical circuit with a single diode (single exponential) is considered as the equivalent photovoltaic cell in the present article. Two different models drawn from the equivalent electrical-circuit are studied: namely four- and five-parameter models. After deciding the model to be used, calculation of the model parameters is the next step. There are basically two approaches to calculate the model parameters. One is numerical, in which the parameters are calculated iteratively, and the second involves the extraction of the parameters analytically [20,21]. The latter approach is used in the present article for extracting the model parameters because it offers simpler but good enough solutions.

The basic model for a photovoltaic module is shown in Fig. 3. The current–voltage (I–V) characteristic of a photovoltaic module can be described with a single diode as

$$I = I_{\mathrm{L}} - I_{\mathrm{o}}\left[\exp\left(\frac{V + IR_{\mathrm{s}}}{N_{\mathrm{s}} n_1 V_{\mathrm{t}}}\right) - 1\right] - \frac{V + IR_{\mathrm{s}}}{R_{\mathrm{sh}}} \tag{1}$$

where I_{L} is the light-generated current (A), I_{o} is the reverse saturation current of the p–n diodes (A), R_{s} is the series resistance of the cells (Ω), R_{sh} is the shunt resistance of the cells

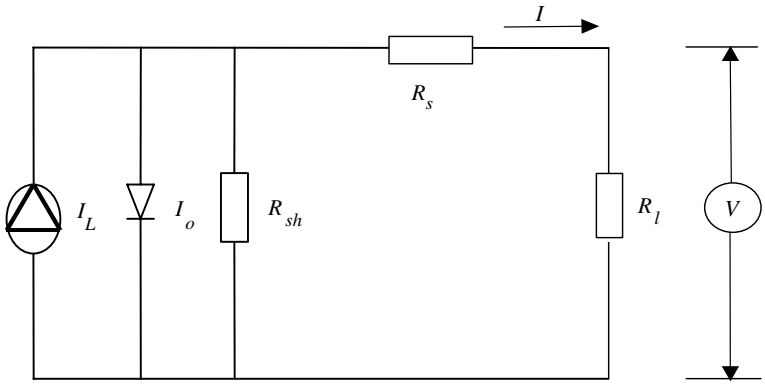

Fig. 3. Equivalent electrical-circuit for a photovoltaic module.

(Ω), N_s is the number of cells in series, n_I is the diode ideality factor, and the product $N_s n_I$ is usually considered a single parameter and denoted as m. V_t is the thermal voltage (V) depending on the cell temperature, which is defined as

$$V_t = kT_c/q \tag{2}$$

where T_c is the cell temperature (K), k is Boltzmann's constant (J K^{-1}), and q is the charge of the electron (C).

The estimation of current and/or voltage of a photovoltaic module is important for accurately estimating the energy production from photovoltaic systems. The power produced by a photovoltaic module depends on the technical characteristics and environmental variables. However, because a model usually consists of only the most important of these technical characteristics and environmental variables, it is almost impossible to obtain a model that accounts for every single effect on the performance of a photovoltaic module. The models generally include parameters that are commonly provided by module manufacturers, such as the electrical performance at standard rating conditions and short-circuit current and open-circuit voltage temperature coefficients [20]. The temperature coefficients for current and voltage at maximum-power point as well as the coefficients describing the effect of air mass, incident angle, and beam and diffuse irradiance are usually avoided in the models as they are not commonly provided by the manufacturers.

3.1. Four-parameter model

Assuming R_{sh} as infinite and neglecting it in Eq. (1), the four-parameter model is obtained as follows:

$$I = I_L - I_o\left[\exp\left(\frac{V + IR_s}{mV_t}\right) - 1\right] \tag{3}$$

The simple relationship of power for a photovoltaic module is

$$P = IV \tag{4}$$

Introducing Eq. (3) into Eq. (4), the power would be

$$P = IV = \left\{ I_{\mathrm{L}} - I_{\mathrm{o}} \left[\exp\left(\frac{V + IR_{\mathrm{s}}}{mV_{\mathrm{t}}} \right) - 1 \right] \right\} V \tag{5}$$

The corresponding cell efficiency is

$$\eta = \frac{P}{G \times A} \times 100 \tag{6}$$

A method to identify the four parameters required for Eq. (3) is summarised by Kou et al. [22]. They treated the product mV_{t} in Eq. (3) as a single parameter and denoted it as a. The short-circuit current can be found when $V = 0$,

$$I_{\mathrm{L,ref}} = I_{\mathrm{sc,ref}} \tag{7}$$

The following equations are used to calculate the other parameters under the reference conditions based on the characteristics of a photovoltaic module:

$$a_{\mathrm{ref}} = \frac{\mu_{\mathrm{V,oc}} T_{\mathrm{c,ref}} - V_{\mathrm{oc,ref}} + E_{\mathrm{q}} N_{\mathrm{s}}}{\frac{T_{\mathrm{c,ref}} \mu_{\mathrm{I,sc}}}{I_{\mathrm{L,ref}}} - 3} \tag{8}$$

$$I_{\mathrm{o,ref}} = \frac{I_{\mathrm{L,ref}}}{\exp\left(\frac{V_{\mathrm{oc,ref}}}{a_{\mathrm{ref}}} \right) - 1} \tag{9}$$

$$R_{\mathrm{s,ref}} = \frac{a_{\mathrm{ref}} \ln\left(1 - \frac{I_{\mathrm{mp,ref}}}{I_{\mathrm{L,ref}}} \right) - V_{\mathrm{mp,ref}} + V_{\mathrm{oc,ref}}}{I_{\mathrm{mp,ref}}} \tag{10}$$

where E_{q} is the band gap energy of silicon (eV) and N_{s} is the number of cells in series in one module. The cell parameters at the operating-cell temperature and solar irradiance are then found from:

$$I_{\mathrm{L}} = \left(\frac{G}{G_{\mathrm{ref}}} \right) [I_{\mathrm{L,ref}} + \mu_{\mathrm{I,sc}} (T_c - T_{\mathrm{c,ref}})] \tag{11}$$

$$I_{\mathrm{o}} = I_{\mathrm{o,ref}} \left(\frac{T_c}{T_{\mathrm{c,ref}}} \right)^3 \exp\left[\left(\frac{E_{\mathrm{q}} N_{\mathrm{s}}}{a} \right) \left(1 - \frac{T_{\mathrm{c,ref}}}{T_c} \right) \right] \tag{12}$$

$$R_{\mathrm{s}} = R_{\mathrm{s,ref}} \tag{13}$$

$$a = a_{\mathrm{ref}} \frac{T_c}{T_{\mathrm{c,ref}}} \tag{14}$$

This model is implemented as follows: Eqs. (7)–(10) are used to find values of the four parameters under reference conditions, which are given in the first row of Table 1. These four parameters are corrected for environmental conditions using Eqs. (11)–(14) and used in Eq. (3), which relates cell current to cell voltage. From Eq. (3) either cell current or voltage could be calculated provided that the other is known. Alternatively, cell current and

Table 1
Examples of parameters at reference and real working conditions and the measured and calculated current values for the four-parameter model at different times on June 29, 2004

Hours:minutes	a (–)	I_{L} (A)	R_{s} (Ω)	I_{o} (A)	I, Measured (A)	I, Calculated (A)
Reference	1.572	7.700	1.233×10^{-2}	1.218×10^{-5}	–	–
08:51	1.621	3.223	1.233×10^{-2}	2.847×10^{-5}	2.964	3.431
12:13	1.725	6.859	1.233×10^{-2}	1.276×10^{-4}	5.858	6.508
17:11	1.685	3.093	1.233×10^{-2}	5.044×10^{-5}	2.882	2.930

voltage could both be calculated at the maximum-power point. Some examples of these four parameters obtained from the available data are presented in Table 1, which consists of three data-points, representing morning, noon and afternoon on June 29. The predicted current values, calculated using these parameters and those measured, are given in the last two columns in Table 1.

As well as the principal power-losses in a solar cell due to light absorption and recombination, another very important loss mechanism that reduces the fill factor and therefore the open-circuit voltage (V_{oc}), is created by the series resistance R_s and the shunt resistance R_{sh} of the solar cell [23]. The series resistance R_s consists of the internal resistance of the solar cell and the contact resistance. Since, with stronger irradiance the current density increases, the power losses at the series resistance also rise. The series resistance of industrially-manufactured solar-cells is expected to be less than 0.50 Ω [19,21,23,24]. The saturation current in the four-parameter model I_o depends on the diffusion coefficient and on the life span of the photo-generated charge carriers outside the space-charge zone [19].

3.2. Five-parameter model

As given in Eq. (1), the five-parameter model is an implicit non-linear equation, which can be solved with a numerical iterative method such as Levenberg–Marquardt algorithm [21]. However, this requires a close approximation of initial parameter values to attain convergence. Alternatively, the parameters may be extracted by means of analytical methods. Some of the analytical methods are studied elsewhere [21,22,25,26]. The following analytical method is used in the present article to extract the parameters [27].

The five parameters I_L, I_o, R_s, R_{sh}, and m are calculated at a particular temperature and solar-irradiance level from the limiting conditions of V_{oc}, I_{sc}, V_{mp}, I_{mp} and using the following definitions of R_{so} and R_{sho}:

$$R_{so} = -\left(\frac{dV}{dI}\right)_{V=V_{oc}} \tag{15}$$

$$R_{sho} = -\left(\frac{dV}{dI}\right)_{I=I_{sc}} \tag{16}$$

where R_{so} and R_{sho} are the reciprocals of the slopes at the open-circuit point and short-circuit point, respectively. The values of these resistances are not usually provided by module manufacturers. R_{so} and R_{sho} values used in the present article are 0.33 and 135 Ω, respectively. Blas et al. [21] suggested R_{so} values between 0.30 and 0.33 Ω and R_{sho} values between 50 and 170 Ω based on the slopes of the experimental curves. The sensitivity analysis of the five-parameter model for R_{so} and R_{sho} revealed that the model predicts current values very well for a wide range of R_{so} and R_{sho} values. Although the improvement was small, the specific values of 0.33 and 135 Ω led to the best prediction of current. A detailed discussion about R_{so} and R_{sho} is given in [21]. The other parameters are calculated as follows. The following equations are used to calculate the five parameters required,

$$I_L = I_{sc}\left(1 + \frac{R_s}{R_{sh}}\right) + I_o\left[\exp\left(\frac{I_{sc}R_s}{mV_t}\right) - 1\right] \tag{17}$$

$$I_o = \left(I_{sc} - \frac{V_{oc}}{R_{sh}}\right)\exp\left(-\frac{V_{oc}}{mV_t}\right) \tag{18}$$

Table 2
Examples of parameters for real working conditions and the measured and calculated current values for five-parameter model at different times on June 29, 2004

Hours:minutes	I_{sc} (A)	V_{oc} (V)	I_L (A)	I_o (A)	R_s (Ω)	R_{sh} (Ω)	m (–)	I, Measured (A)	I, Calculated (A)
08:51	3.227	18.890	3.227	9.334×10^{-9}	0.018	135.0	36.116	2.964	3.125
12:13	6.860	16.948	6.870	1.530×10^{-7}	0.187	135.0	33.948	5.858	6.096
17:11	3.099	17.905	3.110	2.495×10^{-8}	0.005	135.0	35.317	2.882	2.973

$$R_s = R_{so} - \left[\frac{mV_t}{I_o}\exp\left(-\frac{V_{oc}}{mV_t}\right)\right] \tag{19}$$

$$R_{sh} = R_{sho} \tag{20}$$

$$m = \frac{V_{mp} + I_{mp}R_{so} - V_{oc}}{V_t\left[\ln\left(I_{sc} - \frac{V_{mp}}{R_{sh}} - I_{mp}\right) - \ln\left(I_{sc} - \frac{V_{oc}}{R_{sh}}\right) + \left(\frac{I_{mp}}{I_{sc}-\frac{V_{oc}}{R_{sh}}}\right)\right]} \tag{21}$$

where I_{sc} and V_{oc} values at a pair of temperature and solar irradiance levels other than the reference values are calculated as follows:

$$I_{sc} = I_{sc,ref}\frac{G}{G_{ref}} + \mu_{I,sc}(T_c - T_{c,ref}) \tag{22}$$

$$V_{oc} = V_{oc,ref} + mV_t\ln\left(\frac{G}{G_{ref}}\right) + \mu_{V,oc}(T_c - T_{c,ref}) \tag{23}$$

This model is implemented as follows: Eqs. (22) and (23) are used to calculate I_{sc} and V_{oc} from their reference values and at the same time they are corrected for environmental conditions. Eqs. (17)–(21) are used to calculate the five parameters that are in turn used in Eq. (1), which relates cell current to cell voltage. From Eq. (1), the cell current is calculated using the measured voltage values.

The five parameters as well as I_{sc} and V_{oc} values are listed in Table 2 at three data-points, corresponding to different times on June 29. The measured and calculated current values corresponding to these three points are given in the last two columns in Table 2. The parallel or shunt resistance R_{sh} represents the leakage current, which is lost mainly in the p–n interface of the diode and along the edges. Typical values of commercial silicon cells are between 0.1 and 10 Ωm^2. The module manufacturers often give an absolute value in Ω for the shunt resistance [19].

4. Results and discussion

The results of prediction of the operating current from the four- and five-parameter models were analysed for a number of meteorological data-sets. Each set consists of one-day long data, from sunrise to sunset. The important statistics of the meteorological data used are presented in Table 3 for each set. The correlation coefficient R^2 was used as the statistical tool for assessing the performance of the models to predict the current. The R^2 compares the predicted values at each data point to the measured value, thus providing a clear picture of the precision of the model. The R^2 values are given in Table 4 for the four- and five-parameter models for each data-set analysed.

Table 3
Important statistics of the daily data-sets used in the current article

Data set	Date	Irradiance (W/m^2)		Ambient temperature (°C)		Cell temperature (°C)	
		Maximum	Average	Maximum	Average	Maximum	Average
1	June 18, 2004	871.9	489.0	36.6	32.3	54.8	41.2
2	June 29, 2004	930.6	551.0	42.5	35.1	59.9	45.6
3	July 10, 2004	923.1	457.9	41.3	34.5	61.6	42.3
4	July 14, 2004	855.6	476.7	41.0	36.1	57.5	44.4
5	July 15, 2004	894.0	495.2	38.0	34.4	52.0	41.9

Table 4
R^2 of estimate of current by the four- and five-parameter models

Data set	Four-parameter model	Five-parameter model
1	0.995	0.995
2	0.983	0.994
3	0.976	0.986
4	0.990	0.996
5	0.990	0.995

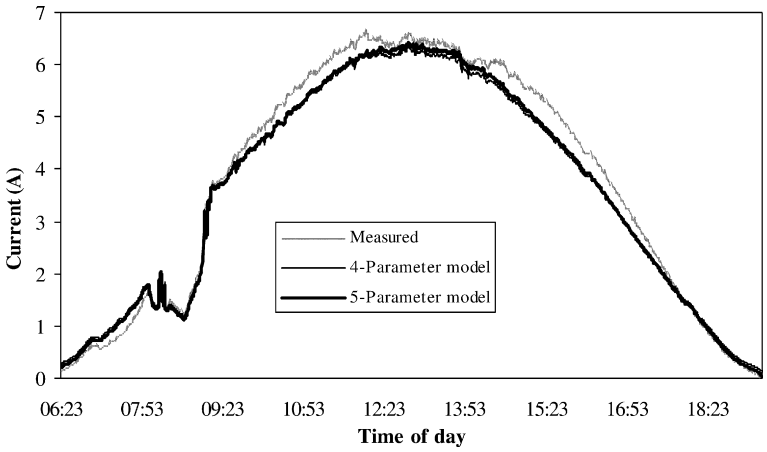

Fig. 4. Current of the photovoltaic module calculated from the four- and five-parameter models versus that measured on June 18, 2004.

The current values calculated from the four- and five-parameter models versus those measured for the first data-set are shown in Fig. 4. Even though the R^2 value for the four-parameter model is equal to that for the five-parameter model, the latter predicts the operating current values around noon, with a smaller error than the four-parameter model does. On that day, both the four- and five-parameter models underestimate the actual current values.

The current values for the second data-set are presented in Fig. 5. As seen in Fig. 5, the current values calculated from the four- and five-parameter models do not show a consistent agreement throughout the day. Both models lead to very close current values until

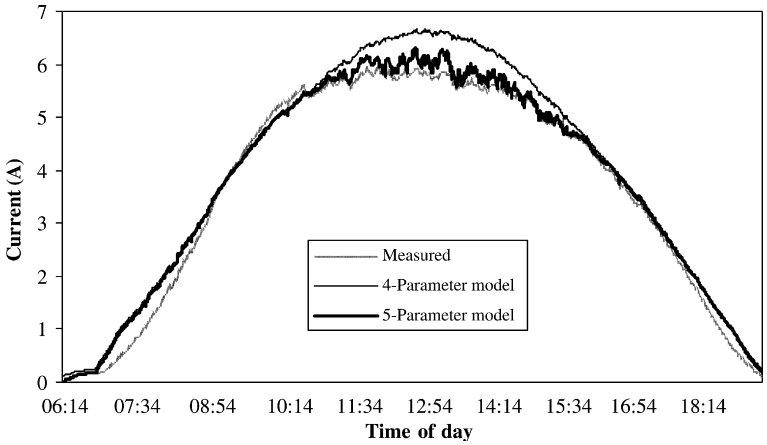

Fig. 5. Current of the photovoltaic module calculated from the four- and five-parameter models versus that measured on June 29, 2004.

around 11 am and after 4 pm. It is also noted that both of the models overestimate the measured current values before 9 am and after 5 pm. Around noon, the four-parameter model overestimates the measured current value with a significant error, while the five-parameter model predicts it with a relatively smaller error.

The current values calculated from the four- and five-parameter models are given in Figs. 6–8 for the rest of the data sets, namely July 10, 14 and 15, respectively. In all of these figures, the four- and five-parameter models provide quite different current values especially around noon, during which the current values calculated from the four-parameter model differ largely from the measured current values. It is observed that the five-parameter model produces relatively closer current values to the measured values around noon. The four-parameter model overestimates the actual current value substantially, while the

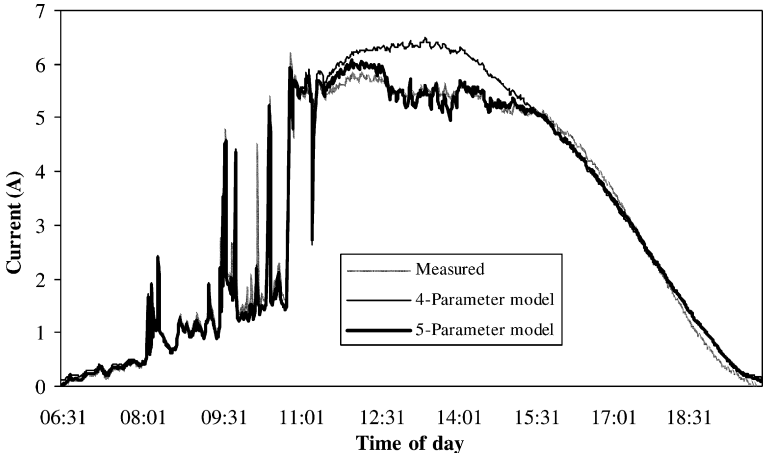

Fig. 6. Current of the photovoltaic module calculated from the four- and five-parameter models versus that measured on July 10, 2004.

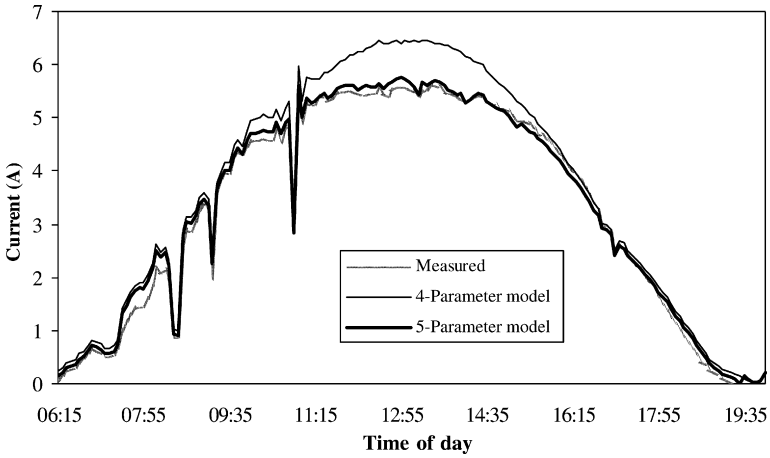

Fig. 7. Current of the photovoltaic module calculated from the four- and five-parameter models versus that measured on July 14, 2004.

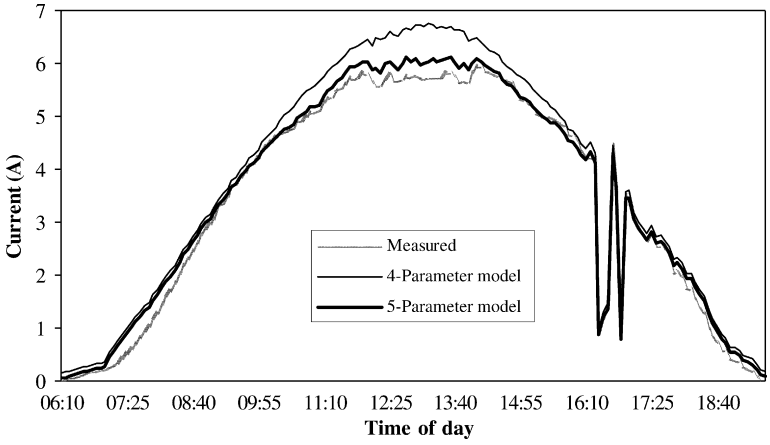

Fig. 8. Current of the photovoltaic module calculated from the four- and five-parameter models versus that measured on July 15, 2004.

five-parameter model slightly overestimates it around solar noon. It is also observed that the four-parameter model almost always overestimates the current throughout the day, substantially so around solar noon. However, the five-parameter model produces both over and underestimations in a single day.

The power produced from the photovoltaic module calculated using the four- and five-parameter models are shown in Fig. 9 together with that measured on July 15. The measured power is estimated by the five-parameter model very closely, while it is estimated by a large error by the four-parameter model around solar noon, when most of the power production occurs. Energy values measured and calculated from the four- and five-parameter models and the error values in estimating the energy are presented in Table 5.

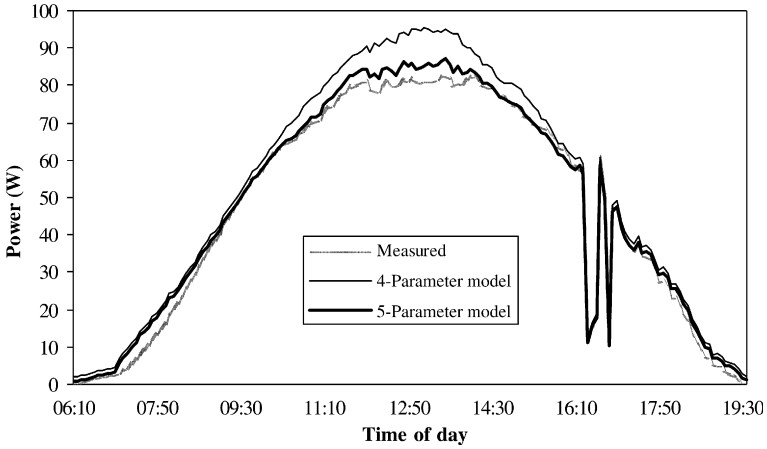

Fig. 9. Power of the photovoltaic module calculated from the four- and five-parameter models versus that measured on July 15, 2004.

Table 5
Energy values measured and calculated from the four- and five-parameter models and the errors in estimating the energy

Data set	Measured energy (Wh/day)	Four-parameter model		Five-parameter model	
		Energy (Wh/day)	Error (%)	Energy (Wh/day)	Error (%)
1	635.05	604.45	−4.82	607.18	−4.39
2	625.30	678.61	8.52	649.15	3.81
3	544.49	578.03	6.16	546.46	0.36
4	605.47	673.05	11.16	618.98	2.23
5	628.45	697.32	10.96	651.62	3.69

5. Conclusions

In the present article, four- and five-parameter analytical models were used to calculate the operating current of a 120 W mono-crystalline photovoltaic module, with the measurements carried out under real working conditions in Iskenderun, Turkey. The most important conclusions drawn from the analysis presented above are:

- R_{so} and R_{sho} values of the five-parameter model are not provided by module manufacturers usually and it is an arduous process to determine their exact values. The sensitivity of this model to both R_{so} and R_{sho} was found to be minor, meaning that the error made was very small for a wide range of R_{so} and R_{sho} values.
- It was seen that the sensitivity of the models to the cell temperature determined their prediction capacity, especially around solar noon, when most of the power is produced in a particular day. The current values estimated, using the four-parameter model, differed most from the measured values around solar noon, when the cell temperature was at its highest level during that particular day. It was shown that the four-parameter model was inadequate in reflecting the cell temperature effect on the current and, therefore, led to a less accurate prediction of current.

- The main conclusion is that, as was indicated by the correlation coefficient R^2 values, the complete five-parameter model led to more accurate current estimations than the simplified four-parameter model, which assumes that the shunt resistance is infinite and thus neglects it.

Acknowledgement

This work has been financed by the Scientific and Technical Council of Turkey (TUBITAK) under Contract no. MISAG-240.

References

[1] Reinhard H. The value of photovoltaic electricity for society. Solar Energ 1995;54(1):25–31.
[2] Aratani F. The present status and future direction of technology development for photovoltaic power generation in Japan. Progr Photovoltaics-Res Appl 2005;13:463–70.
[3] Green MA. Recent developments in photovoltaics. Solar Energ 2004;76:3–8.
[4] Breeze AJ, Schlesinger Z, Carter SA, Tillmann H, Hörhold HH. Improving power efficiencies in polymer–polymer blend photovoltaics. Solar Energ Mater Solar Cells 2004;83(2–3):263–71.
[5] Nierengarten J-F. Fullerene-(π-conjugated oligomer) dyads as active photovoltaic materials. Solar Energ Mater Solar Cells 2004;83(2–3):187–99.
[6] Fanney AH, Dougherty BP. Building integrated photovoltaic test-facility. J Solar Energ Eng 2001;123(2):194–9.
[7] Ahmad GE, Hussein HMS, El-Gheany HH. Theoretical analysis and experimental verification of PV modules. Renew Energ 2003;28:1159–68.
[8] Duke R, Williams R, Payne A. Accelerating residential PV expansion: demand analysis for competitive electricity markets. Energ Policy 2005;33:1912–29.
[9] Martin AG. Price/efficiency correlations for 2004 photovoltaic modules. Progr Photovoltaics-Res Appl 2005;13:85–7.
[10] Celik AN. A simplified model based on clearness index for estimating yearly performance of hybrid PV energy systems. Progr Photovoltaics-Res Appl 2002;10:545–54.
[11] De Soto W, Klein SA, Beckman WA. Improvement and validation of a model for photovoltaic array performance. Solar Energ 2006;80:78–88.
[12] Karatepe E, Boztepe M, Colak M. Neural network based solar-cell model. Energ Convers Manage 2006;47(9–10):1159–78.
[13] Kuo YC, Liang TJ, Chen JF. Novel maximum-power-point-tracking controller for photovoltaic energy-conversion system. IEEE Trans Indust Electron 2001;48(3):594–601.
[14] Meyer EL, van Dyk EE. Development of energy model based on total daily irradiation and maximum ambient temperature. Renew Energ 2000;21:37–47.
[15] Durisch W, Tille D, Worz A, Plapp W. Characterisation of photovoltaic generators. Appl Energ 2000;65:273–84.
[16] Kaygusuz K, Kaygusuz A. Renewable energy and sustainable developments in Turkey. Renew Energ 2002;25:431–53.
[17] Celik AN. Present status of photovoltaic energy in Turkey and life cycle techno-economic analysis of a grid-connected photovoltaic-house. Renew Sust Energ Rev 2006;4:370–87.
[18] Yesilata B, Aktacir A. Investigation of design considerations for photovoltaic water-pumping systems. J Eng Mach 2001;42(493):29–34.
[19] Eicker U. Solar technologies for buildings. New York: Wiley; 2003.
[20] Fanney AH, Dougherty BP, Davis MW. Evaluation building-integrated photovoltaic performance models. In: Proceedings of the 29th IEEE photovoltaic specialists conference (PVSC), New Orleans, LA, USA; 2002. p. 194–9.
[21] Blas MA, Torres JL, Prieto E, Garcia A. Selecting a suitable model for characterizing photovoltaic devices. Renew Energ 2002;25:371–80.
[22] Kou Q, Klein A, Beckman WA. A method for estimating the long-term performance of direct-coupled PV pumping systems. Solar Energ 1998;64(1–3):33–40.

[23] Stutenbaeumer U, Mesfin B. Equivalent model of monocrystalline, polycrystalline and amorphous silicon solar-cells. Renew Energ 1999;18:501–12.
[24] Viorel B. Dynamic model of a complex system including PV cells, electric battery, electrical motor and water pump. Energy 2003;28:1165–81.
[25] Phang JCH, Chan DSH, Philips JR. Accurate analytical method for the extraction of solar-cell model parameters. Electron Lett 1984;20(10):406–18.
[26] Chenlo F, Fabero F, Alonso MC. A comparative study between indoor and outdoor measurements. Final Report of project: testing, norms, reliability and harmonisation. Joule II-Contract N. JOU2-CT92-0178..
[27] Arab AH, Chenlo F, Benghanem M. Loss-of-load probability of photovoltaic water pumping systems. Solar Energ 2004;76(1–3):713–23.